Research on the properties of $ZnO_{1-x}S_x$ thin films modified by sulfur doping for CIGS solar cells*

SUN Hang, XUE Yuming, WANG Luoxin, GUO Qing, and LI Penghai**

School of Integrated Circuit Science and Engineering, Tianjin University of Technology, Tianjin 300384, China

(Received 28 May 2022; Revised 4 July 2022)

$ZnO_{1-x}S_x$ thin films modified by sulfur doping were prepared on glass substrates by chemical bath deposition (CBD) for studying the effect of thiourea concentration on the thin film properties. The obtained $ZnO_{1-x}S_x$ thin films were characterized by scanning electron microscopy (SEM), which shows the surfaces of $ZnO_{1-x}S_x$ thin films deposited under the thiourea concentration of 0.14 M are more compact. X-ray diffraction (XRD) measurement shows that the $ZnO_{1-x}S_x$ thin films with hexagonal crystal structure had strong diffraction peaks and better crystallinity. The optical transmittance of the $ZnO_{1-x}S_x$ thin films with 0.14 M thiourea concentration is above 80% in the wavelength range of 300—900 nm. According to the measurement results from spectrophotometer, the $ZnO_{1-x}S_x$ band gap energy value E_g varies nonlinearly with different S/(S+O) ratio x, and increases with the increase of x. There is a band gap value of 2.97 eV in the $ZnO_{1-x}S_x$ thin films deposited under 0.14 M thiourea concentration. Therefore, the thin films have better structural, optical and electric properties, and are more suitable for the buffer layers of copper indium gallium selenide (CIGS) thin film solar cells.

Document code: A **Article ID:** 1673-1905(2022)11-0678-5

DOI https://doi.org/10.1007/s11801-022-2088-4

For copper indium gallium selenide (CIGS) thin film solar cells, because the large crystal lattice mismatch and the large energy band mismatch between the CIGS absorber layers and the window layers can cause many defects and reduce the photoelectric conversion efficiency of the solar cells if there are no buffer layers between the CIGS layers and the window layers, the buffer layers between the absorber layers and the window layers are used to decrease the two types of large mismatches. Chalcogenide materials have been considered promising buffer layer materials for CIGS solar cells. Compared with the ZnS buffer layer with an optical band gap of 3.71 eV[1], $ZnO_{1-x}S_x$ band gaps are from 2.6 eV to 3.71 eV, and are smaller, which can reduce the two types of mismatches between the CIGS layers and the window layers and improve the photovoltaic performance of the CIGS thin film solar cells. $ZnO_{1-x}S_x$ thin films have many advantages of changeable band gap with different sulfur contents, low cost, rich material and environment friendly, and have been extensively studied[2,3].

The $ZnO_{1-x}S_x$ thin film constitutes the heterojunction together with the CIGS absorption layer and the ZnO window layer. It forms a transition and reduces the band gap step between the CIGS/ZnO layers. The band gap can be changed by combining ZnO with sulfur ions, which shows sulfur ions of relatively large matchable in ZnO has smallest size difference (r_S/r_O=1.3) with oxygen ions[4]. Doping sulfur element changes the band gap from 2.6 eV to 3.6 eV[3]. So, proper adjustment of sulfur element and oxygen element ratio in the $ZnO_{1-x}S_x$ film is conducive to providing a wider transmission rate for the visible light range to improve the photoelectric performance.

Several methods for depositing $ZnO_{1-x}S_x$ films include chemical bath deposition (CBD), sputtering, atomic layer deposition and pulsed laser deposition, etc[5,6]. For such a thin buffer layer, it is difficult to ensure its integrity and compact by evaporation method, while the thin film prepared by CBD method can do. The quality of the thin film prepared by CBD method is affected by the following factors, such as the concentration of reaction solution, temperature and pH value. SAADAT et al[3] concluded that optimizing the sulfur concentration in the buffer layer produced a solar cell with a $ZnO_{0.7}S_{0.3}$ buffer layer with the best efficiency. GHARIBSHAHIAN et al[7] considered that the heterojunction interface mismatch is affected by the carrier concentration and sulfur content of Zn(O, S). As the sulfur content decreases, the impact of the mismatch problem decreases, and the performance of the solar cell is improved.

In recent years, although studies about $ZnO_{1-x}S_x$ thin films have been extensively reported, few researches have been conducted on the effects of thiourea concentration on the morphology, structure, atomic percentage of major

* This work has been supported by the Natural Science Foundation of Tianjin (No.18JCYBJC95400).

** E-mail: orwellx@tjut.edu.cn

elements and optical properties. The variation of $ZnO_{1-x}S_x$ thin films performance for different thiourea concentrations was studied to improve the morphology, structure and optical properties of the films.

The $ZnO_{1-x}S_x$ thin films were prepared by CBD process. However, the Zn^{2+}, O^{2-} and S^{2-} ions in the solution can quickly generate precipitation and affect the growth of the films. Therefore, ammonia as a complex agent was generally added to slow the release rate of metal ions. In addition, ammonium sulfate ($(NH_4)_2SO_4$) was used as a buffer. The NH^{4+} reacted with Zn^{2+} to form a stable complex of $[Zn(NH_3)_n]^{2+}$. The quality of the films were improved with increased ammonia and $(NH_4)_2SO_4$ in the solution, which could controlled the deposition rate of the films.

$ZnSO_4$ were used as the source of Zn^{2+} ions and thiourea as the source of S^{2-} ions. The thiourea concentration in the solution were varied as 0.06 M, 0.10 M, 0.14 M, 0.18 M and 0.22 M to change the proportion of sulfur in the films. To deposit $ZnO_{1-x}S_x$, the 2 cm×4 cm glass substrates were placed into deionized water, 0.02 M zinc sulfate, 0.013 M ammonium sulfate, 25% ammonia water and different thiourea concentrations in beakers. When water bath temperature reached 80 °C, the beakers were placed into the water bath for $ZnO_{1-x}S_x$ deposition. After 80 min of reaction, the glass substrates were taken out from the reaction solutions, washed with deionized water and finally dried with N_2.

The surface morphology of the $ZnO_{1-x}S_x$ thin films were investigated by the ultrahigh-resolution scanning electron microscope with FEG (Verios 460L). The main elemental analysis of the $ZnO_{1-x}S_x$ films was done by energy-dispersive X-ray spectroscopy (EDS) with Quanta FEG 250. X-ray diffraction (XRD) pattern was measured on the crystallization and structure of the films. The optical absorption spectra were obtained by Shimadzu spectrophotometer (UV-3101PC).

In the CBD process, thiourea reacted with OH^- in the reaction solution to form S^{2-}, and S^{2-} and $[Zn(NH_3)_n]^{2+}$ formed $ZnO_{1-x}S_x$ films. Therefore, controlling the concentration of thiourea exerted an influence on the physical structure and optical properties of $ZnO_{1-x}S_x$ films. To study the effect of thiourea concentrations on the surface morphology of obtained polycrystalline thin films, the $ZnO_{1-x}S_x$ thin films deposited at 80 °C for 0.06 M, 0.10 M, 0.14 M, 0.18 M and 0.22 M thiourea concentrations respectively. The obtained $ZnO_{1-x}S_x$ films were characterized by scanning electron microscopy (SEM), as shown in Fig.1.

SEM is typically performed to study morphology of $ZnO_{1-x}S_x$ thin films of five thiourea concentration for analyzing growth mechanism of $ZnO_{1-x}S_x$ thin films. Fig.1(a) shows a significantly incomplete of the $ZnO_{1-x}S_x$ thin film in 0.06 M thiourea concentration. The isolated grains and loose thin films were evident. During the reaction process of the solution, release rate of Zn^{2+} ions in the reaction solution added by complex agent was significantly

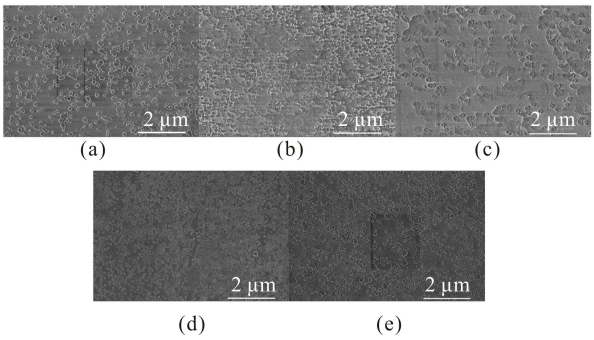

Fig.1 SEM images of the $ZnO_{1-x}S_x$ films for thiourea concentrations of (a) 0.06 M, (b) 0.10 M, (c) 0.14 M, (d) 0.18 M, and (e) 0.22 M

reduced, and the $[Zn(NH_3)_n]^{2+}$ ions generated by Zn^{2+} and NH^{4+} was effectively increased. When the thiourea concentration was 0.06 M, the concentration difference between S^{2-} and Zn^{2+} was small, and the few nucleation sites in the $ZnO_{1-x}S_x$ thin film produced, which was harmful to film growth. For clarity, high-frequency SEM images are shown in Fig.2(a). The crystallinity of $ZnO_{1-x}S_x$ thin film was bad, and grains were nonuniform. Fig.1(b) shows the morphology of $ZnO_{1-x}S_x$ thin film in 0.10 M thiourea concentration. The isolated grains uniformed with 0.10 M thiourea concentration were connected into film. The film exhibited a significantly smaller gaps and more compact than $ZnO_{1-x}S_x$ thin film in 0.06 M thiourea concentration, suggesting that the S^{2-} ions increased by increment of thiourea concentration contributed to increase nucleation sites (Fig.2(b)). However, $ZnO_{1-x}S_x$ thin film still exhibited numerous gaps, indicating it can't provide enough S^{2-} ions for the reaction. When thiourea concentration was increased to 0.14 M, density of $ZnO_{1-x}S_x$ thin film was significantly enhanced, and the $ZnO_{1-x}S_x$ thin film had insignificantly pores. This indicated that the sufficient S^{2-} and $[Zn(NH_3)_n]^{2+}$ could effectively produce uniform nucleation sites, resulting in an accelerating growth rate and more compact of the $ZnO_{1-x}S_x$ thin film. Fig.1(d) shows that the $ZnO_{1-x}S_x$ thin film gradually fragmented in 0.18 M thiourea concentration, while Fig.1(e) shows that the $ZnO_{1-x}S_x$ thin film was completely fragmented with thiourea concentration of 0.22 M. The complete fragmentation of $ZnO_{1-x}S_x$ thin films were attributed to the excessive S^{2-} ions existed in the solution and to the full contact between S^{2-} ions and $[Zn(NH_3)_n]^{2+}$ ions. So, the abundance of nucleation sites was significantly enriched in the $ZnO_{1-x}S_x$ thin films. This resulted in numerous and nonuniform $ZnO_{1-x}S_x$ grains produced by clusters of nucleation sites, which were adhesion on the surface of the $ZnO_{1-x}S_x$ thin films (Fig.2(c)). Owing to the clusters of nucleation sites in the $ZnO_{1-x}S_x$ thin film, they hinder the growth and integrity of the film, which was completely fragmented. The excess carriers with external illumination are injected into the film. The disappearance of excess carriers is mainly completed through the process of disappearing in pairs between electrons and holes. Due to the

increase of pores cause by fragmentation of $ZnO_{1-x}S_x$ thin film, it accelerates the process of the extinction of excess carriers and increases the probability of carrier recombination, and reducing the photoelectric conversion efficiency. Therefore, films with fewer pores and great density are more suitable as buffer layers. Under the condition that the concentration of complex agent remains unchanged, the release rate of Zn^{2+} is slowed down, and the formation of precipitates is reduced. The 0.14 M thiourea is completely hydrolyzed by ammonia, which promotes the reaction between $[Zn(NH_3)_n]^{2+}$ and S^{2-} to form a compact and complete film with reduced holes formation. The $ZnO_{1-x}S_x$ thin films with a thiourea concentration of 0.14 M exhibited the best density (Fig.1(c)).

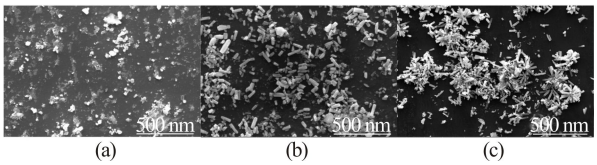

Fig.2 SEM images of the $ZnO_{1-x}S_x$ thin films for thiourea concentrations of (a) 0.06 M, (b) 0.10 M, and (c) 0.22 M at different magnifications

Fig.3 shows the EDS composition distribution images of $ZnO_{1-x}S_x$ films at five thiourea concentrations. The obtained specific elemental chemical compositions measurement results of the EDS composition distribution images with different thiourea concentrations are shown with the atomic percentage in Tab.1. The current study found that with the increase of thiourea concentration, the percentage of S element of the thin films presents a trend of increasing first and then decreasing. For the films grown at the thiourea concentration of 0.14 M, Tab.1 shows the percentage of utmost S element, indicating that thiourea can be hydrolyzed completely to S^{2-}. The release rate of Zn^{2+} ions can be reduced by addition of complex agent, with less precipitation formed. So the $[Zn(NH_3)_n]^{2+}$ reacts extensively with S^{2-} to form $ZnO_{1-x}S_x$. The reaction of $[Zn(NH_3)_n]^{2+}$ with more S^{2-} is ensured, so that the nucleation reaction on the substrate surface can be carried out stably, which reduces the holes formation in the $ZnO_{1-x}S_x$ films. As for the films grown at the thiourea concentration of 0.18 M and above, the excess S^{2-} and Zn^{2+} can generate large $ZnO_{1-x}S_x$ particles faster than the rate of $[Zn(NH_3)_n]^{2+}$ and S^{2-} to form $ZnO_{1-x}S_x$ films. At the same time, the percentage of S element in the films decreases rapidly. Therefore, excess thiourea concentration inhibits films growth. It is confirmed that the growth of thin films is promoted for the enlargement proportion of S/(O+S) in the films.

Fig.4 shows the XRD patterns of $ZnO_{1-x}S_x$ thin films deposited under different thiourea concentrations from 0.06 M to 0.22 M. The patterns in Fig.4 all show the presence of a (106) peak around 31.7° for the films deposited under the thiourea concentrations of 0.10 M, 0.14 M and 0.18 M, which indicates that the films have a wurtzite structure[8]. Furthermore, the XRD patterns for the (106) peaks (Fig.4) reveal a small shift toward lower angles (31.7°<31.819°)[9]. Because of the $ZnO_{1-x}S_x$ thin films with the addition of oxygen element, their lattice constants are smaller than those of the ZnS thin films, which results in a small shift of the (106) peak toward lower angle.

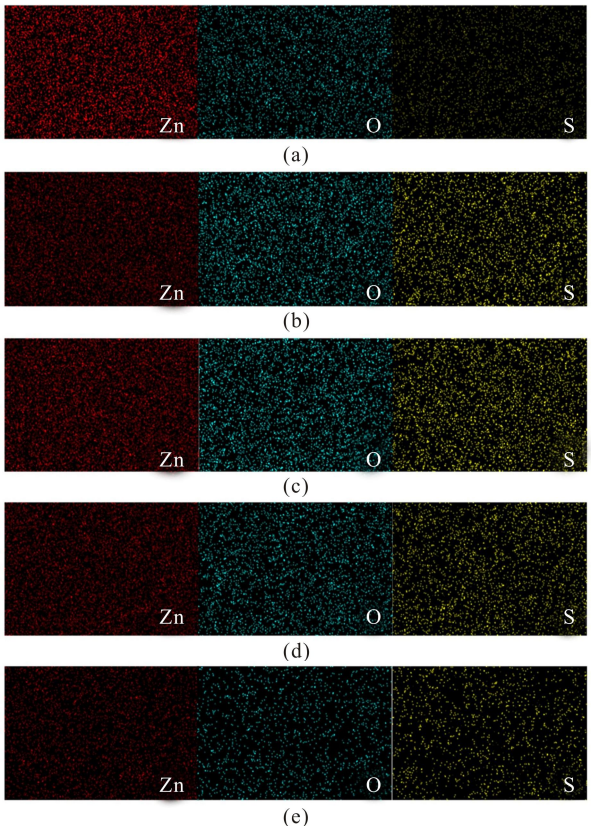

Fig.3 EDS images of $ZnO_{1-x}S_x$ films deposited under different thiourea concentrations of (a) 0.06 M, (b) 0.10 M, (c) 0.14 M, (d) 0.18 M, and (e) 0.22 M

Tab.1 Atomic percentage of each element under different thiourea concentrations

Thiourea concentration (M)	Atomic percentage Zn: O: S	S/(O+S)
0.06	35.42: 50.77: 13.81	0.214
0.10	27.04: 43.90: 29.06	0.398
0.14	29.61: 36.98: 33.41	0.475
0.18	27.83: 49.52: 22.65	0.313
0.22	28.29: 48.62: 23.09	0.322

Fig.5 shows optical absorption curves of the obtained $ZnO_{1-x}S_x$ thin film with thiourea concentrations of 0.06—0.22 M, respectively. The absorbance of the obtained thin films decreased sharply from 300 nm to 350 nm in the wavelength range, and became flat after 400 nm. The absorbance gradually increased with the increase of the thiourea concentration. However, the absorbance almost overlapped between 0.14 M and 0.18 M thiourea concentrations, and decreased with the 0.22 M thiourea concentration. Fig.6 shows the light transmittance curves of thin films with different thiourea concentrations.

The light transmittance of the thin films increased sharply between 300 nm and 370 nm wavelength range, and tended to be flat after 400 nm. The films prepared under the concentrations of 0.10 M and 0.14 M thiourea had good light transmittance, which exceeded 80% in the visible light range.

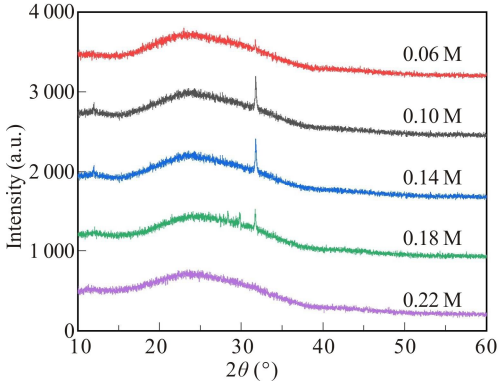

Fig.4 XRD patterns for the $ZnO_{1-x}S_x$ thin films grown under different thiourea concentrations

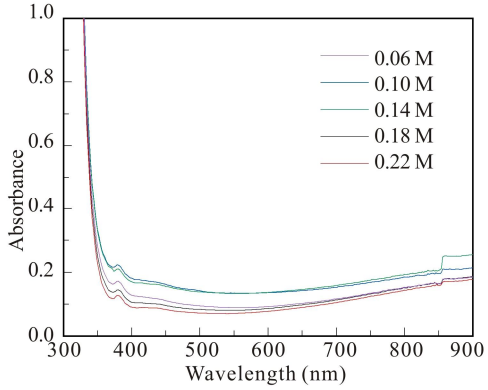

Fig.5 Absorbance vs. wavelength for the $ZnO_{1-x}S_x$ thin films prepared with different thiourea concentrations

The thicknesses of the thin films deposited under 0.06 M, 0.10 M, 0.14 M, 0.18 M and 0.22 M thiourea concentrations are respectively 51.75 nm, 47.87 nm, 53.43 nm, 72.13 nm and 78.13 nm, and the band gap value of Fig.5 was calculated based on absorbance spectra by the following formula and was shown in Fig.7. Fig.7 displayed the $(\alpha hv)^2$-hv plots of the obtained $ZnO_{1-x}S_x$ thin films, which is a direct band gap semiconductor. The E_g value is calculated as follows[10]

$$\alpha hv = A(hv - E_g)^{1/2}. \quad (1)$$

The absorption coefficient α is calculated as follows

$$\alpha = \frac{\ln(T)}{d}, \quad (2)$$

where hv is the energy of photon, E_g is the optical band gap, T is the film transmittance, d is the film thickness, A and α are a band edge constant and the absorption coefficient, respectively. These optical band gaps of $ZnO_{1-x}S_x$ thin films are 3.16 eV, 3.03 eV, 2.97 eV, 3.10 eV and 3.14 eV with 0.06 M, 0.10 M, 0.14 M, 0.18 M and 0.22 M thiourea concentrations, respectively. On enhancing the thiourea concentration in reaction solution, the band gap values were decreased from 3.16 eV to 2.97 eV and then increased to 3.14 eV (Fig.7). This implies that the variation in the band gap values of $ZnO_{1-x}S_x$ thin films as a function of the sulfur doping ratio is a correlation.

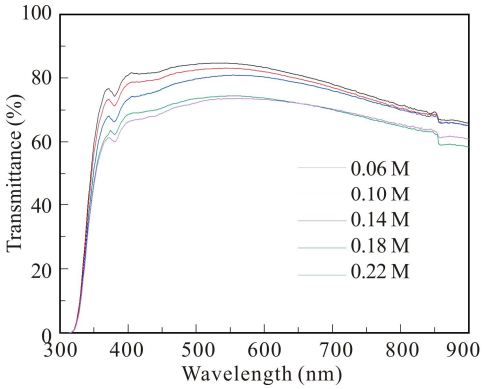

Fig.6 Transmittance vs. wavelength for the $ZnO_{1-x}S_x$ thin films prepared with different thiourea concentrations

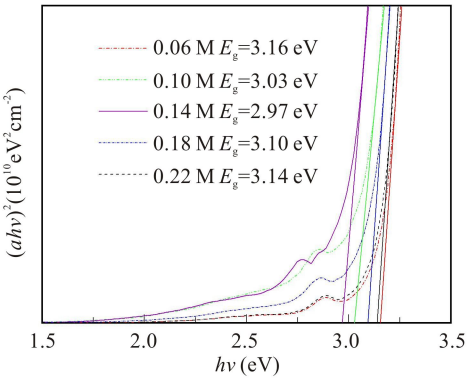

Fig.7 Band gap of $ZnO_{1-x}S_x$ thin films deposited with different thiourea concentrations

To further investigate the dependences of energy band and sulfur content, the fitting curve of the band gap values as a function of the sulfur doping content in the $ZnO_{1-x}S_x$ thin films is shown in Fig.8. x represents the values of S/(O+S) for the $ZnO_{1-x}S_x$ thin films. Fig.6 shows a nonlinear correlation between the band gap values and S/(O+S) ratios of the $ZnO_{1-x}S_x$ films by analyzing the EDS atomic percentage and spectrophotometer[11]. It is well known that the band gap of $ZnO_{1-x}S_x$ is generally described as[12]

$$E_g(ZnO_{1-x}S_x) = xE_g(ZnS) + (1-x)E_g(ZnO) - k(1-x)x, \quad (3)$$

where E_g(ZnS) and E_g(ZnO) represent the band gap values of ZnS and ZnO, and k represents the bowing parameter. By fitting the data of Fig.8 with Eq.(3), the nonlinear equation is expressed as

$$E_g(x) = 1.987x^2 - 1.702\,1x + 3.404\,5. \quad (4)$$

Eq.(4) shows that the band gap is related to the sulfur

composition in different region. This found that in the $0<x<0.8$ region exhibits a significantly smaller band gap value than in the $x=0$ or $x>0.8$ region, which is coincident with the report of PAN et al[11] and MA et al[4]. This result reflects those of MEYER et al[13] who also found that the bowing parameter k is not a constant, which is concerned in the different sulfur composition regions, and optical band gap is changed. In this study, the changing of band gap value E_g results essentially from the giant stress related to the sulfur contents variation and structural defects such as grain boundaries in the polycrystalline films caused by the doping of different thiourea concentrations. Therefore, the results confirmed that the optical band gap value of $ZnO_{1-x}S_x$ thin film can be significantly changed by adjusting sulfur contents. Additionally, owing to the significant band gap difference between the CIGS absorber layer and the ZnO window layer, they are easy to cause lattice mismatch, resulting in numerous defects in the film[14]. Compared with the pure ZnS buffer layer, $ZnO_{1-x}S_x$ can reduce the band gap difference. Such variation in the band gap of the $ZnO_{1-x}S_x$ thin films is critical to the band alignment between absorber/buffer layer.

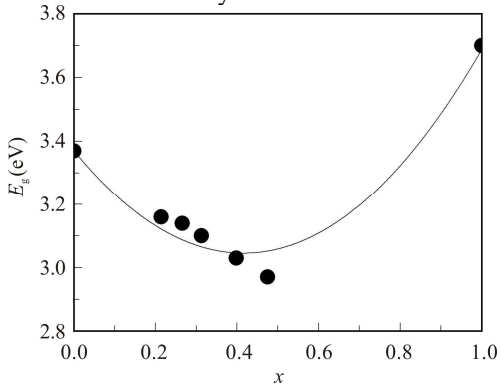

Fig.8 Band gap of $ZnO_{1-x}S_x$ films vs. x

In conclusion, $ZnO_{1-x}S_x$ thin films were prepared using CBD method. The $ZnO_{1-x}S_x$ thin films were characterized by SEM and XRD, the results of which confirmed the preparation of $ZnO_{1-x}S_x$ thin films with a variable morphology, composition and crystallinity at different thiourea concentrations. According to SEM images and XRD pattern, the $ZnO_{1-x}S_x$ thin film at 0.14 M thiourea concentration exhibited good compact and crystallinity. There was a nonlinear relationship between the band gap values and S/(O+S) ratios of the $ZnO_{1-x}S_x$ films by analyzing the EDS atomic percentage and spectrophotometer. It was concluded that the optical properties of the films can be significantly changed by adjusting thiourea concentration. Therefore, considering the crystal quality, homogeneity, and optical band gap, the $ZnO_{1-x}S_x$ thin film obtained at 0.14 M thiourea concentration is likely the appropriate one used as the buffer layer in the CIGS solar cell.

Statements and Declarations

The authors declare that there are no conflicts of interest related to this article.

References

[1] ZELLAGUI R, DEHDOUH H, ADNANE M, et al. $Cd_{1-x}Zn_xS$ thin films deposited by chemical bath deposition (CBD) method[J]. Optik, 2020, 207：164377.

[2] KHEMIRI N, AOUSGI F, KANZARI M. Tunable optical and structural properties of Zn(S, O) thin films as Cd-free buffer layer in solar cells[J]. Materials letters, 2017, 199：1-4.

[3] SAADAT M, AMIRI O, MAHMOOD P H. Potential efficiency improvement of $CuSb(S_{1-x}, Se_x)_2$ thin film solar cells by the Zn(O, S) buffer layer optimization[J]. Solar energy, 2021, 225：875-881.

[4] MA J, TANG K, MAO H, et al. Behavior and impact of sulfur incorporation in zinc oxysulfide alloy grown by metal organic chemical vapor deposition[J]. Applied surface science, 2018, 435：297-304.

[5] WANG Y X, LIU J H, SONG X, et al. Preparation and optical properties of B-doped ZnO thin films[J]. Journal of optoelectronics·laser, 2021, 32(10)：1119-1123. (in Chinese)

[6] BOOSAGULLA D, MANDATI S, MISRA P, et al. Pulse electrodeposited zinc sulfide as an eco-friendly buffer layer for the cadmium-free thin-film solar cells[J]. Superlattices and microstructures, 2021, 160：107060.

[7] GHARIBSHAHIAN I, OROUJI A A, SHARBATI S. Effect of the junction barrier on current-voltage distortions in the Sb_2Se_3/Zn(O, S) solar cells[J]. Optical materials, 2021, 116：111098.

[8] CHENG Q, WANG D, ZHOU H. Electrodeposition of Zn(O, S) (zinc oxysulfide) thin films：exploiting its thermodynamic and kinetic processes with incorporation of tartaric acid[J]. Journal of energy chemistry, 2018, 27(3)：913-922.

[9] SHAN R, YI J, ZHONG J, et al. Effect of sulphur pressure on properties of ZnS thin film prepared by chemical bath deposition technique[J]. Journal of materials science：materials in electronics, 2019, 30(14)：13230-13237.

[10] SHABBIR S, SHAARI A, HAQ B U, et al. First-principles investigations of structural parameters, electronic structures and optical spectra of 5-5 and BeO-type of $ZnO_{1-x}S_x$ alloys[J]. Materials science and engineering B, 2020, 262：114697.

[11] PAN H L, YANG T, YAO B, et al. Characterization and properties of $ZnO_{1-x}S_x$ alloy films fabricated by radio-frequency magnetron sputtering[J]. Applied surface science, 2010, 256(14)：4621-4625.

[12] WANG Y, TIAN F, LI D, et al. First principle studies of $ZnO_{1-x}S_x$ alloys under high pressure[J]. Journal of alloys and compounds, 2019, 788：905-911.

[13] MEYER B K, POLITY A, FARANGIS B, et al. Structural properties and bandgap bowing of $ZnO_{1-x}S_x$ thin films deposited by reactive sputtering[J]. Applied physics letters, 2004, 85(21)：4929-4931.

[14] GHARIBSHAHIAN I, OROUJI A A, SHARBATI S. Efficient $Sb_2(S, Se)_3$/Zn(O, S) solar cells with high open-circuit voltage by controlling sulfur content in the absorber-buffer layers[J]. Solar energy, 2021, 227：606-615.